

# Watching Na Atoms Solvate into $(\text{Na}^+, e^-)$ Contact Pairs: Untangling the Ultrafast Charge-Transfer-to-Solvent Dynamics of $\text{Na}^-$ in Tetrahydrofuran (THF)

Molly C. Cavanagh, Ross E. Larsen, and Benjamin J. Schwartz\*

Department of Chemistry and Biochemistry  
University of California, Los Angeles  
Los Angeles, CA 90095-1569 USA

\*corresponding author: [schwartz@chem.ucla.edu](mailto:schwartz@chem.ucla.edu)

**Abstract:** With the large dye molecules employed in typical studies of solvation dynamics, it is often difficult to separate the intramolecular relaxation of the dye from the relaxation associated with dynamic solvation. One way to avoid this difficulty is to study solvation dynamics using an atom as the solvation probe; since atoms have only electronic degrees of freedom, all of the observed spectroscopic dynamics must result from motions of the solvent. In this paper, we use ultrafast transient absorption spectroscopy to investigate the solvation dynamics of newly-created sodium atoms that are formed following the charge-transfer-to-solvent (CTTS) ejection of an electron from sodium anions (sodide) in liquid tetrahydrofuran (THF). Since the absorption spectra of the sodide reactant and the sodium atom and solvated electron products overlap, we first examined the dynamics of the ejected CTTS electron in the infrared to build a detailed model of the CTTS process that allowed us to subtract the spectroscopic contributions of the sodide bleach and the solvated electron and cleanly reveal the spectroscopy of the solvated atom. We find that the neutral sodium species created following CTTS excitation of sodide initially absorbs near 590 nm, the position of the gas-phase sodium D-line, suggesting that it only weakly interacts with the surrounding solvent. We then see a fast solvation process that causes a red-shift of the sodium atom's spectrum in  $\sim 230$ -fs, a time scale that matches well with the results of MD simulations of solvation dynamics in liquid THF. After the fast solvation is complete, the neutral sodium atoms undergo a chemical reaction, as indicated by the observation of an isosbestic point and the creation of a species with a new spectrum, that takes place in  $\sim 740$  fs. The spectrum of the species created after the reaction then red-shifts on a  $\sim 10$ -ps time scale to become the equilibrium spectrum of THF-solvated sodium atom, which is known from radiation

chemistry experiments to absorb near  $\sim 900$  nm. There has been considerable debate as to whether this 900-nm absorbing species is better thought of as a solvated atom or a sodium cation:solvated electron contact pair,  $(\text{Na}^+, e^-)$ . The fact that we observe the initially-created neutral Na atoms undergo a chemical reaction to ultimately become the 900-nm absorbing species suggests that it is better assigned as  $(\text{Na}^+, e^-)$ . The  $\sim 10$ -ps solvation time we observe for this species is an order of magnitude slower than any other solvation process previously observed in liquid THF, suggesting that this species interacts differently with the solvent than the large molecules that are typically used as solvation probes. Together, all the results allow us to build the most detailed picture to date of the CTTS process of  $\text{Na}^-$  in THF as well as to directly observe the solvation dynamics associated with single sodium atoms in solution.

## I. Introduction

The critical role played by the solvent in solution-phase chemical reactions has prompted a great deal of interest in how a solvent responds to changes in the electronic structure of a reactant or product, a process known as solvation dynamics.<sup>1-8</sup> In most solvation dynamics studies, time-resolved fluorescence<sup>3-5</sup> or various photon echo spectroscopies<sup>6-8</sup> are used to monitor how the solvent relaxes following the change in electronic charge distribution that occurs upon excitation of a dye molecule. The chief difficulty in interpreting such experiments, however, is that excited dye molecules also undergo a significant amount of internal relaxation (e.g., intramolecular vibrational energy redistribution); this internal relaxation is difficult to distinguish from solvation dynamics, particularly since internal relaxation and solvation can occur on similar time scales.<sup>9</sup> One method for avoiding the complexity of having to detangle competing relaxation mechanisms in solvation experiments is to study atomic solutes. Since atoms have no internal degrees of freedom, any spectral relaxation observed following excitation must be due solely to motions of the solvent. Moreover, the sharp electronic resonances of atoms are extraordinarily sensitive to the nature of the interactions with the surrounding media. For example, in rare gas matrices where interactions between the host matrix and dissolved atoms are weak, there is relatively little perturbation in the atom's absorption spectrum from what would be present in the gas phase.<sup>10-12</sup> In polar or strongly interacting solvents, in contrast, a dissolved atom may not even retain its identity, as is the case when Na metal is dissolved in

liquid ammonia to yield sodium cations and solvated electrons.<sup>13</sup> The situation becomes even more interesting when atoms are dissolved in moderately interacting or weakly polar solvents, in which the dissolved species can still be identified as having significant neutral atomic character, but the interactions with the environment completely change the electronic structure and spectroscopy relative to the gas phase.<sup>14-18</sup>

In this paper, we use ultrafast spectroscopy to study atomic solvation in this latter regime; our focus is on watching an initially-prepared gas-phase-like Na atom become solvated in the intermediate-polarity solvent tetrahydrofuran (THF). We chose this solute/solvent system for our study because the spectroscopic properties of both solvated Na atoms and anions in THF have been well studied. For example, the absorption spectrum of solvated Na atoms in THF has been measured both by pulse radiolysis (where solvated Na atoms are created when sodium cations capture injected excess electrons)<sup>19,20</sup> and flash photolysis (where solvated Na atoms are created following photodetachment of an electron via excitation of the charge-transfer-to-solvent band of sodide,  $\text{Na}^-$ ).<sup>21,22</sup> The absorption spectrum of THF-solvated Na atoms, which is shown as the green solid curve in Figure 1,<sup>21</sup> is broad and featureless, peaks near 900 nm, and bears little resemblance to that of Na atoms in the gas phase, where the only significant feature in the visible region is the sharp D-line near 590 nm.<sup>23</sup> The solvated Na atom spectrum is also significantly different from the spectrum of the solvated electron in THF, which peaks near 2100 nm (Figure 1, red dotted curve).<sup>24</sup> This leads to the primary question we address in this paper: Is the THF-solvated Na atom better thought of as a solvated electron whose spectrum is strongly perturbed by the presence of a nearby Na cation or as a neutral sodium atom whose spectrum is strongly perturbed by the surrounding solvent?

One of the reasons it has been so difficult to understand the absorption spectrum of solvated sodium atoms in liquid THF is that they exist only transiently following pulse radiolysis of  $\text{Na}^+$  solutions or following photodetachment from  $\text{Na}^-$ , making them difficult to study with techniques such as electron spin resonance (ESR). ESR experiments have been performed on solvated potassium atoms in THF, however, and the conclusion reached is that the ~1100-nm absorption of the solvated K atom comes from a species with ~36% atomic character.<sup>18</sup> Similar ESR experiments on solvated Rb atoms in other solvents suggest an even higher fractional atomic character,<sup>18</sup> so based on periodic trends one might expect the ~900-nm absorbing solvated neutral Na species to have a lower atomic character than that of potassium. Solvated Cs atoms,

however, can have either more or less atomic character than solvated Rb atoms depending on the solvent,<sup>18</sup> suggesting that the situation is more complicated than would be expected from simple periodic trends. Nevertheless, many radiation and flash photolysis chemists have argued that the ~900-nm absorbing sodium species is best thought of as a sodium atom:solvated electron contact pair, denoted  $(\text{Na}^+, e^-)$ ,<sup>18-21</sup> though there is still debate even in this community.<sup>16,17,22</sup>

In contrast to the pulse radiolysis experiments, ultrafast experiments on sodide in THF have suggested that the 900-nm absorbing species is better thought of as a solvated neutral Na atom. In experiments performed both by our group<sup>25-35</sup> and that of Ruhman and co-workers,<sup>36,37</sup> a gas-phase-like Na atom spectrum peaking near 590 nm was seen immediately following excitation of the ~750-nm charge-transfer-to-solvent (CTTS) band of  $\text{Na}^-$  (Figure 1, blue dashed curve). The ~590-nm absorbing species then disappeared and was replaced on a ~700-fs time scale by the known broad ~900-nm solvated neutral sodium spectrum.<sup>25,26,37</sup> Although neither our group nor Ruhman's was able to assign the nature of the ~900-nm absorbing species based solely on this observation, our group performed additional experiments in which the electron ejected from the parent  $\text{Na}^-$  upon CTTS excitation was re-excited with a second ultrafast laser pulse tuned to ~2100 nm (*cf.* Figure 1).<sup>28,29</sup> We concluded from these experiments that excitation of the detached electron led to formation of ground-state sodide within our ~200-fs instrumental resolution. To us, this suggested that the ~900-nm absorbing species is better thought of as a solvated sodium atom, because if it were instead a contact pair, excitation of one electron would have to induce *both* detached electrons to recombine with the nearby  $\text{Na}^+$  in less than 200 fs, a prospect that we considered unlikely. It is possible, of course, that if the ~900-nm absorbing species were a contact pair with significant atomic character, relatively little motion of the second electron would be required, so that reformation of  $\text{Na}^-$  within 200 fs could still be possible even if the ~900-nm absorbing species were better thought of as  $(\text{Na}^+, e^-)$ .

In this paper, we revisit the question of the nature of the ~900-nm absorbing species by studying its formation following the CTTS photodetachment of  $\text{Na}^-$  in THF. We have chosen experimental conditions similar to those recently published by Ruhman and co-workers<sup>37</sup> that are designed maximize the signal at long times, allowing us to accurately subtract the spectral contributions of both the electron's absorption and the sodide bleach (*cf.* Figure 1). Our experiments lead to a detailed model of the early-time CTTS ejection dynamics that allows us to cleanly extract the spectrum of the solvated neutral sodium species. Our observation of an

isosbestic point leads us to believe that our results provide the first direct evidence that the  $\sim 900$ -nm absorbing solvated neutral sodium species in THF is better thought of as  $(\text{Na}^+, e^-)$ , albeit with a high degree of atomic character. We also find that it takes  $\sim 5$ - $10$  ps for the newly-formed  $(\text{Na}^+, e^-)$  contact pair to fully solvate, a time scale much slower than other solvation processes previously observed in THF.

The rest of this paper is organized as follows. In Section II we present a brief summary of what is known about the ultrafast flash photolysis of  $\text{Na}^-$  in THF. We then proceed in Section III to describe our experimental apparatus as well as the criteria and methods we use to analyze the data in order to cleanly observe the interconversion of Na atoms to  $(\text{Na}^+, e^-)$  in THF. In Section IV we present the data and (along with the Supplemental Information) a detailed discussion of how the data are modeled in order to extract the processes of interest, leading to a new kinetic model for the dynamics following CTTS excitation of  $\text{Na}^-$  in THF that includes the formation of  $(\text{Na}^+, e^-)$  from gas-phase-like neutral Na. We close in Section V with a discussion that we believe explains all of the ultrafast spectroscopic data from both our group and Ruhman's group, including both the early-time CTTS dynamics of  $\text{Na}^-$  and the subsequent interconversion of Na atoms to  $(\text{Na}^+, e^-)$ . In the Appendix, we provide details of the previously-published models<sup>25,26,37</sup> of the ultrafast CTTS dynamics of  $\text{Na}^-$  that are applied in this work and we also describe some of the controversy in the literature over how best to think about the CTTS dynamics of sodide in THF.

## II. Competing Views of the Ultrafast CTTS Dynamics of $\text{Na}^-$

The existence of the sodium anion (and indeed all the alkali anions except Li) in solution has been known since the pioneering work of Dye and co-workers.<sup>38-40</sup> Solutions of  $\text{Na}^-$  are dark blue, the result of an intense electronic absorption in the near IR (*cf.* blue dashed curve, Fig. 1). Studies of how this band shifts as a function of temperature and in different solvents led to the conclusion that the intense  $\text{Na}^-$  absorption is a CTTS transition.<sup>40</sup> Mixed quantum/classical simulations of sodide in water suggest that the broad  $\text{Na}^-$  CTTS absorption band results primarily from transitions between one of the  $3s$  valence electrons bound to the Na nucleus and three, quasi-degenerate  $p$ -like excited states that are bound only by the surrounding solvent cavity;<sup>41</sup> the absorption at higher energies has been ascribed to direct excitation of the  $\text{Na}^-$  valence electrons into the conduction band of the solvent.<sup>30</sup> Polarized pump-probe experiments

by both our group<sup>26</sup> and that of Ruhman and co-workers<sup>36</sup> appear to be consistent with the idea that there are indeed three orthogonally-polarized electronic transitions underlying the Na<sup>-</sup> CTTS band.<sup>42-45</sup> The identity of the higher-energy states as lying in the conduction band, however, recently has been called into question. Quantum molecular dynamics simulations<sup>46,47</sup> and neutron diffraction experiments<sup>48</sup> both suggest that liquid THF naturally contains cavities that are partially-positively polarized and thus predisposed to trap a solvated electron. In particular, the simulations show that the solvent-supported excited states of an electron in THF can lie either in the electron's original cavity (e.g., *p*-like states) or exist either partially or completely in cavities located elsewhere in the solvent.<sup>46,47</sup> Thus, the sodide CTTS absorption band is likely composed of both transitions to *p*-like excited states within the sodide's cavity and transitions to cavities elsewhere in the fluid. We will argue below that the presence of pre-existing cavities in THF has important consequences for the CTTS dynamics of sodide in this solvent.

Because Na<sup>-</sup> provides one of the few examples of an atomic CTTS reaction that is amenable to study by ultrafast laser techniques (I<sup>-</sup> being the other significant example<sup>49-53</sup>), there has been intense interest in its time-resolved spectroscopy both by our group and by Ruhman and co-workers. In the original experiments from our group, we found that the infrared absorption of the detached solvated electrons does not appear instantaneously after excitation, indicative of a delayed ejection mechanism for the CTTS process.<sup>25,26</sup> Once created, the detached electrons recombine with their geminate partners on three distinct time scales, suggesting that they localize at three distinct distances from their parents.<sup>26,28-33,35</sup> We refer to electrons that geminately recombine within ~1 ps as "immediate contact pair" electrons, which presumably lie within the same solvent shell as their geminate partners. We label electrons that recombine in hundreds of ps as residing in "solvent-separated contact pairs", likely one solvent shell away from their geminate partners. Finally, we identify "free" electrons as those that do not recombine on sub-ns time scales, presumably residing far enough from their geminate partners that their subsequent recombination is diffusion controlled. We also found that for excitation on the red side of the Na<sup>-</sup> CTTS band (e.g., at 900 nm), all of the detached electrons reside in immediate contact pairs, but that as the excitation wavelength is tuned to the blue, the fraction of solvent-separated and free electrons produced increases rapidly so that it comprises ~70% of the detached electrons following ~400-nm excitation.<sup>30</sup> Finally, we observed a new absorption near 590 nm that

appears within our instrumental resolution following the CTTS excitation of  $\text{Na}^-$  in many solvents,<sup>25,26,34</sup> which we assigned to the D-line of a “gas-phase-like” Na atom that exists before solvent motions convert this species into the  $\sim 900\text{-nm}$  absorber observed in the earlier studies.<sup>19-22</sup>

Despite all the effort aimed at understanding the ultrafast CTTS dynamics of sodide in THF, there still remains some controversy over many of the details in this deceptively simple system. For example, as described in detail in the Appendix, there is considerable debate concerning the time it takes for the electron to be ejected following the CTTS excitation of sodide. Ruhman and co-workers have speculated that the ejection time is fast and occurs on a sub-200-fs time scale,<sup>36,37</sup> whereas our group has argued that the ejection is delayed, occurring on a slower  $\sim 700\text{-fs}$  time scale.<sup>25-27,29,35</sup> In addition, it is still unknown whether the 900-nm absorbing species produced following CTTS excitation of  $\text{Na}^-$  is better thought of as a solvated gas-phase-like sodium atom or a sodium atom:solvated electron contact pair,  $(\text{Na}^+, e^-)$ . One of the reasons that it has been so difficult to arrive at a consistent picture of the  $\text{Na}^-$  CTTS process is that several kinetic processes – the initial CTTS detachment, dynamic solvation, and the recombination of detached electrons in immediate contact pairs – all take place on very similar time scales. Moreover, the spectra of the  $\text{Na}^-$  reactant and the sodium atom product strongly overlap (*cf.* Fig. 1), making it difficult to cleanly separate the solvation and recombination dynamics of the sodium atom from the bleach/recombination dynamics of the  $\text{Na}^-$  CTTS band.

To aid in detangling these dynamics, in this paper we have elected to revisit the transient spectroscopy of  $\text{Na}^-$  in THF following  $\sim 400\text{-nm}$  excitation, an excitation wavelength where the amount of fast recombination is minimal. In addition to re-investigating the dynamics in the visible region already explored by Ruhman and coworkers,<sup>37</sup> we also present new data in the near and mid-IR regions that allow us to directly observe the dynamics of both the neutral sodium species and the solvated electron at wavelengths at which there is minimal spectral overlap (*cf.* Figure 1). What we will show is that in the visible spectral region where both we and Ruhman and co-workers have probed, our two data sets are essentially identical. Thus, as we demonstrate explicitly in the Supplementary Information, the differing conclusions between our group and that of Ruhman and co-workers do not come from a conflict of data but rather from a difference in interpretation. What follows is our attempt to resolve the conflict of interpretation by incorporating the near- and mid-IR spectral transients as well as the visible data

into the modeling, allowing us to present the most complete picture of the electron detachment and solvation dynamics that occur following the CTTS excitation of  $\text{Na}^-$  in THF.

### III. Experimental and Data Analysis Methods

As with the work described in our previous papers,<sup>25-35</sup> we fabricated samples of  $\text{Na}^-$  in freshly distilled liquid THF using a modification of the technique originally published by Dye.<sup>40</sup> Our method started by placing a small piece of sodium metal and a small piece of potassium metal in a 0.5-mm path length quartz spectrophotometer cell along with  $\sim 0.5$  ml of a solution of  $\sim 1:1000$  v/v 15-crown-5 ether/THF. The cell was then agitated by sonication, creating a sodide sample with an optical density of  $\sim 2$  at the 750-nm CTTS absorption maximum. These samples were stored at  $\sim -20$  °C and used only while the optical density of the sample at its absorption maximum remained above 1.0. A typical sample prepared using this method lasted for several weeks.

The details of our femtosecond pump-probe setup also have been published previously.<sup>54</sup> Briefly, the experiments were performed using a regeneratively-amplified Ti:Sapphire laser from Spectra Physics that produces pulses of  $\sim 120$ -fs duration with  $\sim 800$ - $\mu\text{J}$  of energy at a 1-kHz repetition with a central wavelength of 790 nm. The amplified beam was split into  $\sim 200$ - $\mu\text{J}$  and  $\sim 600$ - $\mu\text{J}$  portions; the low-energy portion was doubled in a BBO crystal and attenuated to produce 395-nm,  $\sim 0.2$ - $2$ - $\mu\text{J}$ , excitation pulses that were focused to a  $\sim 0.25$ -mm spot, and the high-energy portion was used to pump an optical parametric amplifier (OPA) to create tunable signal and idler pulses in the 1.2 – 2.4  $\mu\text{m}$  region. For experiments probing between 480 nm and 760 nm, probe pulses were created by either frequency doubling the signal beam or by sum frequency mixing the signal or idler beams with the remaining 790-nm fundamental light. For experiments probing near 1100 nm, the probe pulses were taken directly from the OPA signal beam. For experiments probing near 2000 nm, the probe pulses were taken directly from the OPA idler beam. The wavelength of the probe light was measured using an Ocean Optics fiber-based spectrometer with  $\sim 5$ -nm resolution. No matter how they were created, the probe pulses were directed onto a computer-controlled translation stage that produced a controlled variable time delay relative to the pump pulse. A small portion of the probe beam was split off before the sample and sent to a reference detector, and the data were double-normalized (the intensity of the signal probe pulse was divided by that of the reference probe pulse both with and without the

pump pulses present) on a shot-by-shot basis, allowing us to collect transient signals as small as  $\Delta OD \sim 10^{-4}$  with a few hours of signal averaging.<sup>54</sup> For all of the ultrafast spectral transients reported below, the relative pump-probe polarization was set to the magic angle and the experiments were performed at room temperature. The error bars we report represent the 95% confidence limit based on the collection of multiple consecutive data sets.

To better characterize the temporal response of our instrument when 395-nm excitation is employed, we used a Si wafer as a sample to measure the cross-correlation of our pulses for what we expect to be the wavelength combination with the worst time resolution, 395-nm pump/2200-nm probe. Assuming that the transient absorption rise of the Si sample was instrument-limited, fitting this data gave a 330-fs Gaussian (full width at half maximum) for the cross-correlation. We expect the cross-correlation using visible probe wavelengths to have as good or better time resolution than this for two reasons. First, the visible probe pulses were created via non-linear processes from the IR signal or idler beams from the OPA, so we expect the visible pulses to have a shorter duration than the pulses from which they were created. Second, the group velocity mismatch between the pump and probe pulses is the greatest when the wavelength difference between them is the greatest; there should be much less group velocity mismatch between the 395-nm pump and visible probe pulses than there is with a mid-IR probe pulse.

Since our double-normalization scheme allows us to collect data from only a single probe wavelength at a time, the fact that the pump-probe overlap changes with each probe wavelength makes it difficult to compare the absolute signal intensities from one probe wavelength to the next. Thus, to model the data, our transient signals had to be scaled to have the correct relative intensities. To do this, we fit each spectral transient to a sum of four to eight exponentials (as needed to assure a good fit) convoluted with a Gaussian representing our instrument function; this fit provided a means for interpolating the data between the measured time points as well as furnished an analytic representation that could be used in the modeling.<sup>55</sup> As explained further below in Section IV.B, we modeled the data by assuming that the  $\text{Na}^-$  bleach, the solvated electron and the solvated neutral sodium species each had its equilibrium spectrum (Figure 1) 30 ps after the excitation pulse. For each wavelength, we averaged the measured signal intensities between 29 and 39 ps delay and scaled them to match the sum of the known neutral sodium atom,  $\text{Na}^-$ , and solvated electron extinction coefficients at that wavelength (with the  $\text{Na}^-$  extinction coefficient taken as negative to account for its ground-state bleach). Our choice to do

this scaling at  $\sim 30$ -ps delay is important since as we show below, the solvation of the sodium atom is not complete for  $\sim 25$  ps. Incorrectly assuming that the sodium atom's spectrum is equilibrated before this time leads to errors when modeling the data,<sup>37</sup> as discussed in more detail in the Supplementary Information.

We note that care must be used in choosing the precise  $\text{Na}^-$  and solvated electron equilibrium spectra to use for scaling the relative intensities of the spectral transients. For  $\text{Na}^-$ , this is a direct result of the fact that it is quite difficult to obtain a clean equilibrium spectrum. The difficulty arises because scattering can contaminate the blue side of the absorption spectrum and the presence of a small amount of dissolved  $\text{K}^-$  can contaminate the red side of the spectrum.<sup>21,22</sup> Thus, for our modeling, we chose to use the Gaussian-Lorentzian fits to the  $\text{Na}^-$  spectrum published by Seddon and co-workers,<sup>21</sup> who found that these fits worked well in modeling their photo-bleaching experiments. In addition, we found that it was not adequate to use the standard Gaussian-Lorentzian fit that has been reported for the solvated electron's spectrum.<sup>24</sup> Although the standard Gaussian-Lorentzian fit works well in the infrared near the maximum of the electron's absorption spectrum, it significantly underestimates the absorption cross-section in the visible,<sup>22,24</sup> a region that is critical for understanding the spectral dynamics of the neutral sodium atom. Thus, for scaling the data in our analysis, we scanned and digitized the raw absorption spectrum of the solvated electron published in Figure 2 of Reference 24 and scaled these values to the known electron absorption cross-section.<sup>24,56</sup> Despite these difficulties with the spectrum of  $\text{Na}^-$  and the solvated electron, however, we feel confident using the published Gaussian-Lorentzian fits to the neutral sodium atom spectrum,<sup>21</sup> since this fit accurately reproduces the spectrum obtained in both flash photolysis<sup>21</sup> and pulse radiolysis<sup>20</sup> experiments.

#### **IV. Results: Extracting the Solvation Dynamics of the Sodium Atom Following the CTTS Excitation of $\text{Na}^-$ in THF**

In this section, we present the results of femtosecond pump-probe experiments studying the transient spectroscopy following CTTS excitation of  $\text{Na}^-$  in THF. We excite the  $\text{Na}^-$  CTTS transition at 395 nm and probe at wavelengths spanning 480 nm to 2200 nm. Because the spectra of the  $\text{Na}^-$  bleach, the solvated electron and the solvated sodium atom overlap (Figure 1), to cleanly extract the dynamic spectroscopy of the sodium atom created upon CTTS excitation,

we must first understand the spectral dynamics of both the  $\text{Na}^-$  bleach and the detached solvated electron. Thus, we begin in Section IV.A with a detailed examination of the detached electron's spectral dynamics in the infrared region of the spectrum. We will show that the solvated electron's spectrum undergoes no spectral shift following detachment, so that the spectral kinetics of the detached electron in the visible region are straightforward to model. In Section IV.B, we then use this information, along with the assumption that there is no spectral diffusion in the bleach of the  $\text{Na}^-$  CTTS band when the pump and probe relative polarization is at the magic angle, to detangle the overlapping spectral dynamics in the visible region of the spectrum. We then divide out the population of sodium atoms as a function of time, allowing us to clearly observe the interconversion of the initially-prepared gas-phase-like Na atom that absorbs at 590 nm into the  $\sim 900$ -nm absorbing solvated neutral sodium species. We conclude in Section IV.C by presenting a new kinetic model based on the data that describes the interconversion and solvation processes that take place as the gas-phase-like sodium atom reacts to form a  $(\text{Na}^+, e^-)$  contact pair.

#### A. *The (Lack of) Solvation Dynamics of the Detached CTTS Electron:*

As discussed above, in order to properly detangle the visible spectral transients following the CTTS excitation of  $\text{Na}^-$ , it is important to understand the details of the electron detachment process. The questions we address in this subsection are: What is the ejection time for the solvated electron? And once the electron is ejected, what are its subsequent spectral dynamics? To answer these questions, we chose to study the solvated electron's formation and subsequent spectral evolution by probing at multiple wavelengths in the  $\sim 2000$ -nm region, where the solvated electron is the *only* absorbing species.<sup>57</sup> Figure 2 shows the results of experiments where we excited  $\text{Na}^-$  in THF at 395 nm and varied the probe wavelength throughout the region where the electron is the sole absorber. The figure shows clearly that the spectral kinetics are identical at every probe wavelength. This indicates that there are no dynamical processes that change the shape of the detached electron's spectrum; instead, the transients in Figure 2 directly reflect the time evolution of the *population* of detached electrons. A simple fit of the traces in Figure 2 to our Delayed Ejection (DE) Model,<sup>25,26,58</sup> which is described in more detail in the Appendix, yields an appearance time for the solvated electron of  $\sim 400$  fs. We will discuss the difference between this time and the  $\sim 700$ -fs time obtained in our original fits to the DE<sup>25</sup> and

the Delayed Ejection Plus Solvation (DE+S)<sup>26</sup> models below in Section V. From our fit we also determine that ~32% of the electrons geminately recombine with their neutral sodium partners within the first two picoseconds, a result that matches well with previously published data at this pump wavelength.<sup>30</sup>

In addition to the data in Fig. 2, which shows that there is no dynamic solvation of the detached electron following 395-nm CTTS excitation of  $\text{Na}^-$ , we also showed in a previous publication<sup>27</sup> that there is no solvation of the electron following 790-nm CTTS excitation of  $\text{Na}^-$ . There are two main reasons why it could be considered surprising that both 395-nm and 790-nm excitation yield equilibrated electrons following a delayed ejection. First, experiments probing the CTTS dynamics of iodide found clear evidence for solvation of the detached electron with a time that was fast in water and slower in longer-chained alcohols.<sup>52</sup> Moreover, as shown below in Section IV.B, there is significant solvation of the sodium atom during the CTTS process, both before and after the reaction to form the  $(\text{Na}^+, e^-)$  complex. Thus, if electron solvation in THF were similar to ion solvation, we would expect any electron solvation dynamics following CTTS detachment from  $\text{Na}^-$  to be slow enough to be clearly observed with our time resolution. Second, if the ejection of the CTTS electron is indeed delayed, one would expect that prior to ejection (as suggested by Ruhman and coworkers<sup>36,37</sup>) the excited electron would significantly perturb the 590-nm absorption of the neutral sodium species. The similarity of the initially-created sodium atom's absorption to its gas-phase D-line, along with the fact that its spectrum is independent of both pump wavelength and solvent,<sup>25,26,34,36,37</sup> suggests that the excited CTTS electron is not correlated with its parent sodium atom. So, if the excited CTTS electron is not immediately detached but is also not correlated with the sodium atom immediately after excitation, where is it?

To answer this question, it is important to have a detailed understanding of the nature of the molecular packing in liquid THF. Molecular dynamics simulations have shown<sup>46,47</sup> (and neutron diffraction experiments have confirmed<sup>48</sup>) that liquid THF is a naturally porous solvent that contains many relatively large cavities. Not only are these cavities about the right size to contain an equilibrated solvated electron, but the packing of the THF molecules around these cavities gives them a net positive electrostatic potential: thus, liquid THF is full of pre-existing traps where an excess electron would already be close to equilibrium.<sup>46-48</sup> To better understand how the presence of these cavities affects solvated-electron localization dynamics, we performed

nonadiabatic mixed quantum/classical simulations of the photoexcitation of the solvated electron in liquid THF.<sup>47</sup> We found that depending on the excitation energy, the initially-created excited state of a solvated electron can be confined to its original cavity, have amplitude in both its original cavity and one of the nearby pre-existing cavities (which we refer to as a disjoint state), or lie mostly in one of the pre-existing cavities.<sup>46</sup> Thus, when a THF-solvated electron is excited, it has the opportunity to move to a new place in the liquid without having to carve out a new cavity; instead, dynamic solvation can lead to localization of the excited-state wavefunction into a different cavity from which it originated, and the subsequent radiationless decay places the electron back on its ground state in a new location in the fluid that is almost entirely equilibrated. Indeed, our simulations showed clearly that the little solvation that does occur after the electron reaches its ground state is faster than the dynamics of relocalization that take place while the electron is excited.<sup>47</sup>

We believe that the presence of pre-existing traps for a solvated electron in liquid THF can explain all of the observed behavior following CTTS excitation of  $\text{Na}^-$ . Like the solvated electron in THF, the excited states of  $\text{Na}^-$  likely consist not only of solvent-supported *p*-like states supported by the original  $\text{Na}^-$  cavity, but also disjoint states that share significant amplitude with nearby pre-existing cavities. Excitation of  $\text{Na}^-$  places the electron in one of these excited states, where it is no longer correlated with the electron(s) remaining on the neutral sodium atom. Following excitation, it takes  $\sim 450$  fs for dynamic solvation and to localize the excited electron either into the original cavity or into one of the pre-formed cavities, as we had measured previously in a three-pulse delayed multiphoton ionization experiment.<sup>27</sup> The excited electron then undergoes internal conversion to the ground state to finally detach into its new, essentially pre-equilibrated home. This explains the delayed appearance of the solvated electron's spectrum, the fact that the electron appears with its equilibrium absorption spectrum (Figure 2), and the fact that the 590-nm absorption of the Na atom does not depend on the wavelength used to excite the  $\text{Na}^-$  CTTS band.<sup>37</sup> The dependence of the electron ejection distance on excitation wavelength<sup>27-30,32,33,35</sup> also can be simply explained by considering the nature of the initially-prepared excited state: the higher the excitation photon energy, the more likely the initially-occupied excited state is to have disjoint character<sup>47</sup> and thus the more likely the electron is to ultimately detach into one of the pre-existing cavities (to form what we refer to as solvent-separated contact pairs and free electrons) instead of into the original cavity (to form

what we refer to as immediate contact pairs). Water and other polar solvents do not contain the pre-existing cavities that are present in liquid THF, which explains why the detached electrons undergo significant spectral evolution in these solvents as they work to carve out their new cavities following CTTS excitation.

Overall, the dynamics of the detached electron following CTTS excitation of  $\text{Na}^-$  are relatively simple to understand. The formation of the detached electrons is delayed, and for the 395-nm excitation that we have used here,  $\sim 30\%$  of the detached electrons form in immediate contact pairs and undergo recombination on a  $\sim 1$ -ps time scale; the remaining electrons detach into solvent-separated contact pairs or as free electrons, which recombine on much longer time scales. Since the detached electrons appear at equilibrium, it is straightforward to model their spectral dynamics in the visible: at every visible wavelength, the detached electrons' transient spectroscopy must be identical to that observed in the infrared (Figure 2).

*B. The Interconversion of Gas-Phase-Like Na atoms into ( $\text{Na}^+, e^-$ ):*

Now that we have a detailed understanding of the detached CTTS electron's transient spectroscopy, we can investigate the spectral dynamics of the Na atom created following CTTS excitation. Figure 3 shows a subset of the 33 spectral transients that we collected using a 395-nm pump wavelength and probe wavelengths spaced every  $\sim 10$  nm between 480 nm and 760 nm; the solid curves through the data are fits to multi-exponentials convoluted with a Gaussian representing the instrument response, as described in Section III. The figure shows that the spectral dynamics throughout this region are quite complex: most of the transients show non-monotonic dynamics with multiple rises and decays on several different time scales. This complexity results from the fact that  $\text{Na}^-$ , the blue tail of the detached solvated electron, and the neutral sodium atom created upon CTTS excitation all absorb in this wavelength region (*cf.* Figure 1), and that each of these different species has distinct spectral dynamics. Fortunately, the spectral dynamics of both the  $\text{Na}^-$  bleach and the solvated electron can be accounted for in a straightforward manner, allowing us to subtract away their contribution to the data in Figure 3 and thus cleanly observe the spectral dynamics of the neutral sodium atom.

To perform this subtraction of the bleach and electron contributions to the data in Figure 3, we start with the fact that the observed signals must be due to absorption from the neutral

sodium atom, the solvated electron, and the bleach of the  $\text{Na}^-$  CTTS transition. Knowing this, the measured signal at each probe wavelength can be scaled and written as:

$$\Delta OD(\lambda, t) = P_{\text{Na}^0}(t)\varepsilon_{\text{Na}^0}(\lambda, t) + P_{e^-}(t)\varepsilon_{e^-}(\lambda) - P_{\text{Na}^-}(t)\varepsilon_{\text{Na}^-}(\lambda) \quad (1)$$

where  $\Delta OD(\lambda, t)$  is the net time-dependent extinction coefficient at probe wavelength  $\lambda$ ,  $P_i(t)$  is the dynamical population of species  $i$  as a function of time (scaled at long times as described in Section III), and  $\varepsilon_i(\lambda)$  is the wavelength-dependent extinction coefficient of the equilibrium spectrum of species  $i$  (*cf.* Figure 1). We expect the absorption spectrum of the neutral sodium atom,  $\varepsilon_{\text{Na}^0}(\lambda, t)$ , to vary with time due to dynamic solvation, since both our group and Ruhman and coworkers have observed the  $\text{Na}^0$  absorption near 590 nm convert into the  $\sim 900$ -nm absorbing species. We argued above in Section IV.A that the solvated electron should have its equilibrium spectrum,  $\varepsilon_{e^-}(\lambda)$ , at all times following excitation, and we assume that the bleach of the  $\text{Na}^-$  CTTS band also should have its equilibrium spectrum,  $\varepsilon_{\text{Na}^-}(\lambda)$ , at all times when the pump and probe polarizations are at the magic angle.<sup>59,60</sup> We also argued in Section IV.A that the electron population,  $P_{e^-}(t)$ , can be directly obtained from the measured absorption dynamics in the  $\sim 2000$ -nm region shown in Figure 2. Thus, to unravel the  $\text{Na}^0$  component of the observed spectroscopy, we need only to determine the bleach population,  $P_{\text{Na}^-}(t)$ . Unlike the solvated electron, there is no region of the spectrum where we can cleanly probe the  $\text{Na}^-$  bleach without interference from one of the other absorbing species (*cf.* Figure 1). Thus, we modeled the bleach dynamics by assuming that the magic-angle polarized bleach appeared instrument-limited, and that the bleach recovered at exactly the same rate that the solvated electrons disappeared due to recombination. In essence, we are assuming that  $P_{\text{Na}^-}(t)$  is given by the DE<sup>25</sup> or DE+S model<sup>26</sup> using the measured solvated electron dynamics in the  $\sim 2000$ -nm region (Figure 2; see the Appendix for more detail on the DE and the DE+S models).<sup>58</sup> Figure 4 shows our DE/DE+S fit to the electron population (upper panel) and the corresponding time-dependent bleach population derived from the DE/DE+S model (lower panel). Finally, to scale the overall intensity of each of the measured single-wavelength transients in Figure 3 correctly, we assumed (as described in Section III) that all of the species produced, including the solvated sodium atom, had their equilibrium absorption spectrum 30 ps after excitation. We also used the fact that the population of sodium atoms,  $P_{\text{Na}^0}(t)$ , and the population of detached electrons,  $P_{e^-}(t)$ , are equal to the population of bleached  $\text{Na}^-$ , as dictated by stoichiometry.

Thus, armed with the data in Figure 3, the time-dependent populations  $P_e(t)$  and  $P_{\text{Na}^-}(t)$  obtained from the traces shown in Figure 4, and the equilibrium absorption spectra  $\epsilon_e(\lambda)$  and  $\epsilon_{\text{Na}^-}(\lambda)$  given in Figure 1, we can use Eq. 1 to extract the time-dependent absorption contribution of the neutral sodium atoms,  $\epsilon_{\text{Na}^0}(\lambda, t) P_{\text{Na}^0}(t)$ , which is shown in Figure 5. Although the data shown in Figure 5 is similar to that presented in Reference 37, all of the subsequent analysis and conclusions that we present below are quite different from those in Ref. 37. In the Supplementary Information, we present a detailed comparison between our analysis and that used by Ruhman and coworkers in Ref. 37 to make clear how different assumptions in the modeling lead to the extraction of different time-dependent spectra for the solvated neutral sodium atom created following the CTTS excitation of  $\text{Na}^-$  in THF. When constructing the spectra in Figure 5, it is important to note that the time resolution of the pump-probe traces shown in Figure 3 is likely to be somewhat better than the time resolution of the IR scans shown in Figure 2, making direct subtraction of the extracted bleach kinetics (Figure 4) during the pump-probe overlap problematic. For this reason, we have chosen not to show any data at times prior to  $\sim 0.4$  ps, so that all the reconstructed spectra we present are safely outside the pump-probe cross-correlation. Fortunately, as discussed further below, none of the conclusions we draw depend on dynamics that take place faster than our worst-case time resolution.

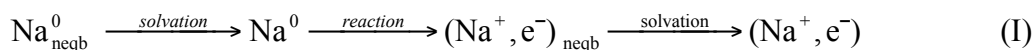
Since stoichiometry dictates that the population of solvated neutral sodium atoms must be equal to the number of excited sodium anions, we can take the data in Figure 5 and further extract the solvated sodium atom's time-dependent spectrum,  $\epsilon_{\text{Na}^0}(\lambda, t)$ , by dividing out the time-dependent population,  $P_{\text{Na}^0}(t) = P_{\text{Na}^-}(t)$ , as shown in Figure 6.<sup>61</sup> Figure 6A shows an expanded view of the earliest-time dynamics, where it is clear that the strong early-time absorption of the Na atom at  $\sim 590$  nm, which we had originally assigned to the gas-phase-like Na D-line,<sup>25,26</sup> is split into three peaks. A similar observation was also made by Ruhman and coworkers,<sup>37</sup> who ascribed this splitting to weak interactions with the solvent that exist before the newly-created sodium atom becomes solvated. They suggested that the initial appearance of the absorption at 590 nm is not reflective of a gas-phase environment but is instead more akin to the absorption of a weakly-solvated Na atom, as in a low-temperature rare gas matrix.<sup>10,11,37</sup> Figure 6A also makes it clear that as time progresses and the solvent begins to relax, the spectrum of the initially-created non-equilibrated Na atom begins to red-shift, particularly on the red edge of the band.

For us, the real surprise comes at later times, from  $\sim 1.4$  to  $\sim 2.1$  ps, shown in Figure 6B, where the presence of an isosbestic point near 710 nm indicates that a chemical reaction takes place. The presence of this isosbestic point is a clear sign that there are two chemically distinct species in co-existence, and that the interconversion between these two species is a kinetic process and is not due to simple dynamic solvation. After the interconversion is complete, Figure 6C shows that the newly-created chemical species undergoes an additional red-shift due to solvation over the next  $\sim 10$  ps, and it is not until  $\sim 25$  ps that the  $\sim 900$ -nm equilibrium spectrum of the solvated neutral sodium species (Figure 1) is finally established. We note that the 710-nm isosbestic point is visible only over the limited time range shown in Figure 6B because both the initially-created 590-nm absorbing species and the species produced after the reaction undergo solvent-induced spectral shifts. Fortunately, as discussed in more detail in Section V, the solvation of the initially-created species occurs faster than the chemical interconversion time, and the solvation of the species produced after the reaction occurs much more slowly than the interconversion time, providing a time window outside of both solvation processes in which the isosbestic point can be observed.

The presence of the isosbestic point seen in Figure 6B, which is indicative of a chemical reaction in which the  $\sim 590$ -nm absorbing weakly-solvated sodium atom converts into the known  $\sim 900$ -nm neutral sodium atom absorption, has profound implications for the assignment of the  $\sim 900$ -nm absorbing species. The observation of the isosbestic point makes it difficult to assign the  $\sim 900$ -nm absorption to a solvated neutral sodium atom: if the 900-nm absorbing species were a solvated neutral sodium atom, we would expect the solvent relaxation that converts the  $\sim 590$ -nm absorbing species to the  $\sim 900$ -nm absorbing species to be smooth, without any signatures of a chemical reaction. Thus, the isosbestic point suggests that the most likely identity of the 900-nm absorbing species is a tightly-bound sodium cation/solvated electron contact pair,  $(\text{Na}^+, e^-)$ , as had originally been suggested by the radiation chemistry community.<sup>18-21</sup> The observed isosbestic point is thus a signature of the reaction taking place to form  $(\text{Na}^+, e^-)$  from a weakly-solvated Na atom. This suggests that the motions of the solvent that cause the valence electron remaining on the sodium atom to partially detach to form the contact pair comprise a chemical process distinct from the solvation initiated by ejection of the original CTTS electron. The “ejection” of the second valence electron, however, can only be partial, as evidenced by the fact that the  $(\text{Na}^+, e^-)$  spectrum is very different from that of a free solvated electron (*cf.* Figure

1) and by the fact that excitation of the CTTS detached electron can induce *both* of the former valence electrons to reattach to the  $\text{Na}^+$  core within  $\sim 200$  fs.<sup>28,29</sup> Thus, the data in Figure 6 strongly indicate that the  $\sim 900$ -nm absorption of the species with the stoichiometry of a neutral sodium atom is best thought of as a  $(\text{Na}^+, e^-)$  contact pair with a high degree of neutral atomic character.

Overall, the data in Figure 6 suggest that a new model is needed to describe the spectral kinetics of the Na atom produced upon the CTTS excitation of  $\text{Na}^-$  in THF. We introduce the following scheme to describe the formation of the equilibrium  $(\text{Na}^+, e^-)$  contact pair:



where the subscript neqb indicates that a species has not been equilibrated by the solvent. We turn in the next section to a discussion of the spectroscopy and kinetics of each of the species and processes in Scheme I. In combination with the ideas presented above and in the Appendix, this scheme will allow us to build a complete picture of all of the dynamics associated with the CTTS excitation of  $\text{Na}^-$  in THF.

### C. A New Kinetic Model for the Formation of $(\text{Na}^+, e^-)$ from $\text{Na}^0$

Given that the data in Figure 6 suggest that the Na atom created following the CTTS excitation of  $\text{Na}^-$  in THF follows Scheme I, our goal in this section is to obtain the individual spectra of the  $\text{Na}_{\text{neqb}}^0$ ,  $\text{Na}^0$ ,  $(\text{Na}^+, e^-)_{\text{neqb}}$  and  $(\text{Na}^+, e^-)$  species and the rate constants for the interconversion between them. Since the data in Figure 6 suggest that the solvation of  $\text{Na}_{\text{neqb}}^0$  to produce  $\text{Na}^0$  is relatively fast and that the solvation of  $(\text{Na}^+, e^-)_{\text{neqb}}$  to produce  $(\text{Na}^+, e^-)$  is relatively slow, the data at intermediate times, from 1.4 to 2.1 ps, provide the best window to view the spectral changes associated with the reaction that converts  $\text{Na}^0$  into  $(\text{Na}^+, e^-)_{\text{neqb}}$ . To investigate these spectral changes, we applied singular-valued decomposition<sup>62</sup> (SVD) analysis to the spectra between 1.4 and 2.1 ps presented in Figure 6B. In our analysis, we assumed that there were only two distinct absorbing species that interconverted with single-exponential kinetics; the details of our SVD analysis are presented in the Supplementary Information. The results of our SVD analysis, shown in Figure 7, give the individual spectra of both  $\text{Na}^0$  (blue dashed curve) and  $(\text{Na}^+, e^-)_{\text{neqb}}$  (red solid curve) as well as a rate constant of  $(740 \text{ fs})^{-1}$  for the interconversion between the two species. Figure 6C and the SVD analysis make it clear that the  $(\text{Na}^+, e^-)_{\text{neqb}}$

species is formed far from equilibrium. In addition, the equilibrated  $\text{Na}^0$  species' spectrum still shows the same three-peak splitting, suggesting that even after solvent relaxation, this species is still best thought of as interacting weakly with the solvent.

Now that we have a good handle on the spectroscopy and formation kinetics of  $(\text{Na}^+, e^-)_{\text{neqb}}$  from  $\text{Na}^0$  via our SVD analysis, our next goal is to investigate the solvation dynamics associated with the relaxation of  $\text{Na}^0_{\text{neqb}}$  into  $\text{Na}^0$ . To cleanly isolate the  $\text{Na}^0$  species, we subtracted the  $(\text{Na}^+, e^-)_{\text{neqb}}$  spectrum in Figure 7, weighted by the exponential rise determined from the SVD analysis, from the data in Figure 6 prior to 2.1 ps; examples of the corrected spectra are shown in the inset of Figure 8. To extract a characteristic solvation time from this data, we calculated the average frequency,  $\langle \tilde{\nu} \rangle$ , of the  $\text{Na}^0$  spectra at each time using:<sup>63</sup>

$$\langle \tilde{\nu} \rangle = \frac{\int_0^\infty \tilde{\nu} I(\tilde{\nu}) d\tilde{\nu}}{\int_0^\infty I(\tilde{\nu}) d\tilde{\nu}} \quad (2)$$

The behavior of the average frequency for the solvation of  $\text{Na}^0_{\text{neqb}}$  is shown in Figure 8; it fits reasonably well to a single-exponential decay with a time constant of  $\sim 230$  fs. This solvation time for the relaxation of  $\text{Na}^0_{\text{neqb}}$  to  $\text{Na}^0$  is only slightly faster than the 430-fs relaxation component seen in earlier studies of the solvation dynamics associated with excitation of the dye Coumarin 153 in liquid THF.<sup>4</sup>

Finally, using the spectrum and time scales obtained from the SVD analysis in Figure 7, we also can subtract the spectrum of the solvated  $\text{Na}^0$  species from the data in Figure 6 at times between 1.4 and 45 ps to unravel the spectroscopy associated with the solvation of  $(\text{Na}^+, e^-)_{\text{neqb}}$  to form  $(\text{Na}^+, e^-)$ . Since our data set does not extend far enough into the infrared to allow us to see the low-energy side of the contact pair's absorption, we fit the high-energy side of the spectra at each time to a Lorentzian function.<sup>64</sup> We forced the oscillator strength of the Lorentzian to be the same as it is for the Lorentzian half of the 900-nm absorbing equilibrated sodium atom (thus fixing the amplitude of each Lorentzian) but allowed the width and maximum energy of each Lorentzian to vary independently. Figure 9 shows the time dependence of the best-fit Lorentzian widths and maximum energies along with exponential fits to each of these changing parameters. Figure 9 makes clear that the changes in both the spectral maximum and width fit very well to single exponentials, with decay times of  $\sim 5.9$  ps for the spectral maximum and  $\sim 9.7$  ps for the width. The surprise from this analysis is that the solvation of the contact pair is so slow; the time

scale is an order of magnitude slower than any other dynamic process associated with the CTTS excitation of  $\text{Na}^-$ .

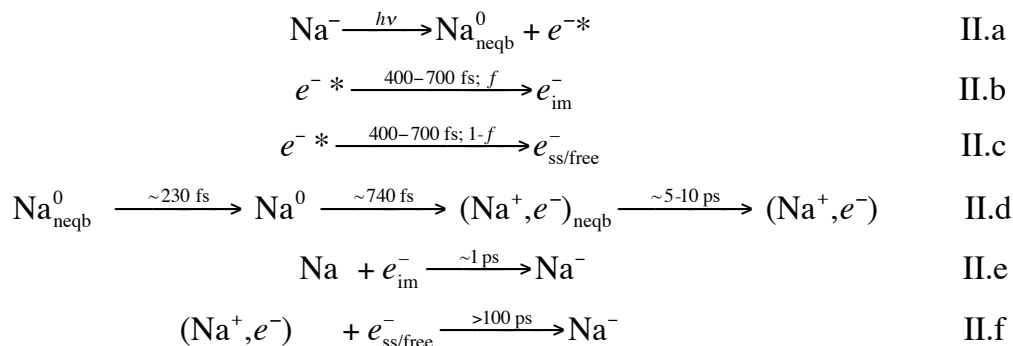
To further investigate this slow solvation process of the contact pair, we performed additional experiments exciting the CTTS band of  $\text{Na}^-$  at 395 nm and probing near 1100 nm, a wavelength that allowed us to look at the absorption of the sodium atom (and solvated electron) without any contribution from the bleach of the  $\text{Na}^-$  ground state; the data are shown in Figure 10A. Fortunately, we have a detailed understanding of the (lack of) spectral dynamics of the solvated electron (see section IV.A), so it is straightforward to subtract off the electron's spectral contribution to this transient; the results of this subtraction are shown in Figure 10B. The rise of the corrected absorption in Figure 10B, which should cleanly reflect the appearance of the solvated ( $\text{Na}^+, e^-$ ) contact pair, fits well to a  $\sim 5.5$ -ps exponential, a time that is consistent with the spectral shift deduced from our Lorentzian fits.<sup>65</sup> The slow rise evident in Figure 10B confirms that the long-time solvation of  $(\text{Na}^+, e^-)_{\text{neqb}}$  that we observed in Figures 6C and 9 is not an artifact of our data analysis. Instead, all of the visible and near-IR data clearly support a picture in which the newly-produced non-equilibrated contact pair undergoes slow cooling on a  $\sim 5$ – $10$ -ps time scale.

## V. Discussion: A New Understanding of the $\text{Na}^-$ CTTS Reaction in THF

In this paper, we have presented a detailed exploration of the ultrafast spectroscopy following the CTTS excitation of  $\text{Na}^-$  in room-temperature THF. We find that the ejection of the CTTS electron is delayed and that there is no evidence for solvation of the electron following detachment (Figure 2). The fact that the detached electrons are formed essentially at equilibrium is consistent with the idea that the detachment process involves a radiationless transition that causes the excited electron to relocalize and relax into one of the pre-existing cavities that are a natural feature of liquid THF.<sup>46–48</sup> The sodium atom left behind upon excitation of the CTTS electron initially absorbs at  $\sim 590$  nm (Figure 6, dark purple curve (0.38 ps)) and shows the characteristic peak splitting that reflects weak interactions with the surrounding solvent.<sup>10,11,37</sup> This unequilibrated Na atom is solvated on a  $\sim 230$ -fs time scale, although it remains in a weakly-interacting environment, as evidenced by the fact that the relaxed Na atom spectrum at  $\sim 1.4$  ps still shows some evidence of the characteristic peak splitting (Figure 7, blue dashed curve). The solvated Na atom then undergoes a solvent-induced chemical reaction, converting into a non-

equilibrated sodium atom/solvated electron contact pair (albeit one with a large degree of neutral atomic character) on a  $\sim 740$ -fs time scale. Once the reaction is complete, the non-equilibrated contact pair (Figure 7, red solid curve) solvates slowly, and the  $\sim 900$ -nm equilibrium spectrum of this species (Figure 1, green solid curve) appears on a  $\sim 10$ -ps time scale.

All of these processes can be represented by the following straightforward kinetic model:



where  $e^{-*}$  in Scheme II represents the CTTS-excited electron before it has made the nonadiabatic transition to detach and reach its ground state,  $f$  is the fraction of electrons ejected into immediate contact pairs, and Na in step II.e represents the sodium atom at any stage of step II.d. This scheme is more complex than the DE+S model (shown in the Appendix) because in this model the relaxation dynamics of the electron are independent of the dynamics of the sodium atom, which undergoes two solvation processes and a chemical reaction. Scheme II provides what we believe is the best kinetic representation of all the processes that occur following the CTTS excitation of  $\text{Na}^-$  in THF.

The kinetic scheme presented above shows how the nature of the solvent is what determines each aspect of the CTTS process. For example, it is the fact that THF contains pre-existing traps for solvated electrons<sup>46-48</sup> that we believe leads to the electron appearing with its equilibrium spectrum even though the Na atom undergoes significant solvent cooling, both before and after its reaction to form  $(\text{Na}^+, e^-)$ . The fact that the Na atom does undergo a spectral shift is not all that surprising: the solvent structure has to rearrange from one initially optimized for negatively-charged ground-state sodide to one more appropriate for a neutral species. Moreover, the neutral sodium atom left behind upon CTTS excitation is significantly smaller than the parent anion, so that solvent molecules must translate inward to fill the void formerly occupied by the larger sodide anion. Our group has performed classical molecular dynamics simulations of precisely this process, and found that inertial translational and rotational motions

of liquid THF accommodate a small neutral atom created from a larger atomic anion with an inertial Gaussian time scale of  $\sim 260$  fs,<sup>66</sup> very similar to the  $\sim 230$ -fs solvation time scale that we observed experimentally (Figure 8).

Our experiments also revealed that the reaction that converts the sodium atom into the  $(\text{Na}^+, e^-)$  contact pair takes place on a 740-fs time scale, a time that we had mistakenly assigned as a solvation process in our original DE+S model.<sup>26</sup> It is only the presence of a complete data set, including the detailed information concerning the electron's spectral dynamics in the infrared, that has allowed us to uncover the spectral signatures of this reaction and assign the  $\sim 900$ -nm absorbing species as a tightly-bound contact pair. It is also interesting to note that the reaction time we measure is quite similar to the  $\sim 700$ -fs time scale we had assigned to the detachment of the CTTS electron. This suggests that our original assignment of the electron ejection time as being  $\sim 700$  fs might be in error: this time was based on fits to the DE+S model that relied on data in the visible region, so that the time scale we assigned to electron detachment was influenced by the unrelated interconversion process that also occurs on a similar time scale. Figure 2 clearly shows, however, that the formation of the detached electron is delayed (and slower than the  $< 200$ -fs time scale suggested by Ruhman and coworkers<sup>36,37</sup>); our fit of the mid-IR data to the DE model (not including any of the visible data) shown in Figure 2 yields a detachment time of  $\sim 400$  fs. This  $\sim 400$ -fs time could be the actual appearance time of the electron, or it may be a convolution of a slower detachment time with an instrument-limited absorption from the CTTS electron's excited state (which has a clear spectral signature in the 1100-1500 nm region).<sup>26,36,57</sup> Our previous three-pulse experiments put a *lower* limit of  $\sim 450$  fs on the electron detachment time,<sup>27</sup> so the data presented here are entirely consistent with a delayed detachment of the CTTS electron in  $\sim 450$  to 700 fs.

Once the reaction to form the contact pair is complete, the final process that takes place following the CTTS excitation of  $\text{Na}^-$  is cooling of  $(\text{Na}^+, e^-)_{\text{neqb}}$  to form the 900-nm absorbing  $(\text{Na}^+, e^-)$  on the relatively slow  $\sim 5$ -10 ps time scale. Both our group<sup>25,26</sup> and that of Ruhman and coworkers<sup>36</sup> missed this slow solvation step in our earlier work because we chose to excite the  $\text{Na}^-$  CTTS transition at 780 nm, where  $\sim 90\%$  of the detached electrons are ejected into immediate contact pairs and recombine within  $\sim 1$  ps, thus washing out the signatures of any long-time dynamic solvation.<sup>67</sup> The fact that recombination can disrupt this final solvent relaxation step suggests that equilibrium  $(\text{Na}^+, e^-)$  contact pairs are likely never formed following

the low-energy excitation of  $\text{Na}^-$  since the parent sodide is reformed before the non-equilibrated contact pair ever has time to solvate.

Why is the solvation of  $(\text{Na}^+, e^-)_{\text{neqb}}$  so slow?<sup>68,69</sup> Even though we expect that liquid THF prefers to accommodate solvated-electron-like objects,<sup>46-48</sup> in this case the solvent must rearrange from packing around a centrosymmetric, non-dipolar object to a non-centrosymmetric object that presumably has a fair-sized dipole moment. Moreover, the solvation of the newly-created contact pair likely involves not just a change in the distribution of charge but also a large shape change (the electron side of the contact pair grows as the sodium cation side shrinks) that would require extensive translational reorganization of the solvent molecules. We also speculate that slow solvation could be explained by the lack of a large driving force for formation of the contact pair. If the driving force is small then the process takes place only when the correct solvent fluctuation occurs, which could explain the slow time scale observed for this process if the required fluctuation is rare. A definitive assignment of which solvent motions are responsible for the slow cooling of  $(\text{Na}^+, e^-)_{\text{neqb}}$  awaits simulations. In future work, we will study the solvation of  $(\text{Na}^+, e^-)$  after attachment of an electron created via CTTS detachment of  $\text{I}^-$  to a nearby solvated sodium cation; this alternative method for producing the contact pair leads to a blue-shifting spectrum during equilibration rather than the red-shifting spectrum observed in the lower panel of Figure 6.<sup>70</sup>

We close our discussion by considering the implications of the slow cooling of  $(\text{Na}^+, e^-)$  for the interpretation of our previous three-pulse experiments. We had originally assigned the ~900-nm absorption as arising from a solvated neutral sodium atom rather than a contact pair because we had found that excitation of solvent-separated electrons at ~2000 nm led to an instrument-limited (<200 fs) recovery of the  $\text{Na}^-$  at 490 nm, and we felt that it was unlikely that two detached electrons could both recombine with a sodium cation so quickly when only one was excited.<sup>28,29</sup> It is possible though, that what we had detected within 200 fs was not the equilibrated  $\text{Na}^-$  species but rather an unsolvated  $\text{Na}^-$ . If this were the case, there could still be some structural rearrangement around the re-formed sodide that occurs after the initial formation of the unsolvated  $\text{Na}^-$  species. Also, in our experiments we chose to re-excite solvent-separated electrons that were produced only ~6 ps after the initial CTTS excitation;<sup>29</sup> thus, these electrons were likely not excited in the presence of fully-solvated  $(\text{Na}^+, e^-)$  but instead were excited in the presence of partially-solvated  $(\text{Na}^+, e^-)_{\text{neqb}}$ . Since we expect the solvent environment around

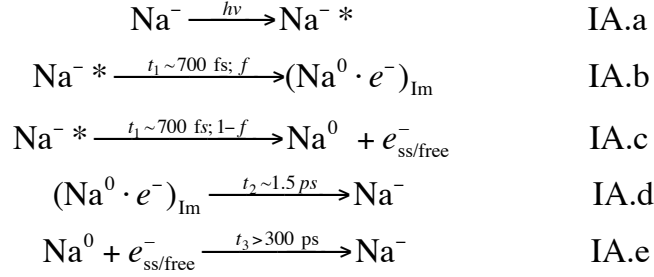
$(\text{Na}^+, e^-)_{\text{neqb}}$  to be closer to that of the parent  $\text{Na}^-$  than that of the equilibrated contact pair, it is possible that the reason re-excitation of the CTTS electron led to the rapid loss of the  $\text{Na}^-$  bleach at 490 nm is only because the newly-formed contact pair had not yet had enough time to equilibrate. It is interesting to speculate on what might be different if we had elected to re-excite the CTTS electrons after the cooling of  $(\text{Na}^+, e^-)$  was complete (30 ps or more after the initial excitation). Would the excitation-induced recombination, as measured by the 490-nm bleach recovery, be shut off partially or completely? Or would it still occur, but only after a significant time delay due to the need to completely rearrange the solvent around the now-stabilized contact pair? Based on the results presented above, we plan to revisit our 3-pulse experiments to address exactly this question; the answers should provide further insights into the atomic character of the  $(\text{Na}^+, e^-)$  contact pair as well as the nature of the CTTS dynamics of  $\text{Na}^-$ .

**Acknowledgements:** This work was supported by the National Science Foundation under Grant CHE-0603766. We would like to thank Dr. Arthur E. Bragg for helpful discussions about the data analysis, Dr. Arthur E. Bragg and Ryan M. Young for assistance with the experiments, and Ian M. Craig for helpful discussions concerning the SVD analysis.

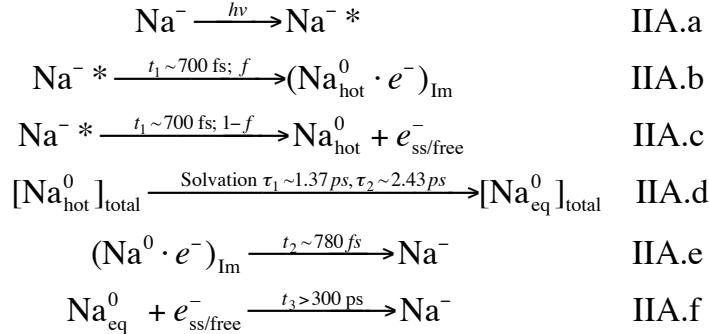
### **Appendix: Controversy and Competing Models for the Ultrafast CTTS Dynamics of $\text{Na}^-$**

As discussed in the text, the ultrafast CTTS dynamics of  $\text{Na}^-$  in THF have been studied by both our group and that of Ruhman and co-workers, with each of our groups presenting different interpretations of the data and different models to explain the observed dynamics. In this Appendix we present a brief review of the controversy, and we also outline the kinetic models that both our group (including the DE and DE+S models used to fit the electron population data and bleaching dynamics in Figure 4) and Ruhman's group have presented to describe the basic processes that take place in this system.

Based on our original ultrafast pump-probe experiments on sodide in THF, we proposed a detailed kinetic model to explain the observed  $\text{Na}^-$  CTTS dynamics, which we referred to as the “delayed ejection” (DE) model (Scheme IA).<sup>25</sup>



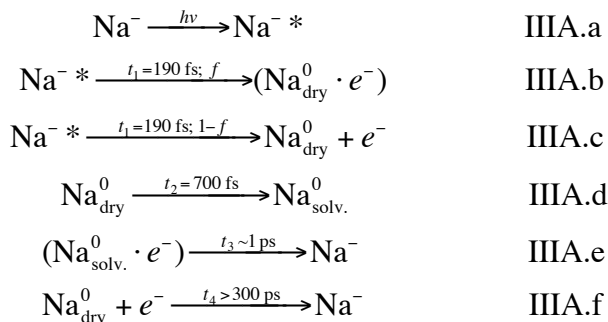
where  $f$  is the fraction of detached electrons that form immediate contact pairs,  $(\text{Na}^0 \cdot e^-)_{\text{Im}}$ , and  $1-f$  is the fraction that form solvent-separated or free sodium atoms ( $\text{Na}^0$ ) and electrons ( $e^-_{\text{ss/free}}$ ).<sup>71</sup> Although the DE model was able to reproduce most of the pump-probe spectral transients,<sup>25</sup> the equations derived from this scheme are clearly inadequate to describe the entire CTTS process because they assume that every species appears with its equilibrium absorption spectrum. Thus, to account for the fact that the neutral sodium species is produced out of equilibrium with its solvent environment, we subsequently extended the model to include dynamic solvation, which we referred to as the “delayed ejection plus solvation” (DE+S) model (Scheme IIA).<sup>26</sup>



where solvation was modeled by fitting the  $\text{Na}_{\text{hot}}^0$  spectrum to a Gaussian-Lorentzian band whose central frequency and width shifted exponentially with time constant  $\tau_1$  and whose oscillator strength decayed exponentially with time constant  $\tau_2$  to reach the equilibrium spectrum,  $\text{Na}_{\text{eq}}^0$  (Figure 1). We found that the DE+S model was able to satisfactorily account for the dynamics observed with multiple pump and probe wavelength combinations in a variety of different solvents.<sup>26</sup> Moreover, the DE+S model provided a statistically significant improvement over the DE model, suggesting that solvation of the sodium atom plays an important part in the physics of the  $\text{Na}^-$  CTTS reaction.

More recently, Ruhman and co-workers revisited the visible ultrafast CTTS dynamics of  $\text{Na}^-$  in THF, and based on the results of their experiments, they proposed a slightly different

model to explain the observed spectral transients, which they referred to as “Model 2” (Scheme IIIA).<sup>37</sup>



In their paper, Ruhman and co-workers made a detailed comparison between their Model 2 and our original DE model (which they refer to as Model 1), and argued that Model 2 fits the data in the visible region better than the DE model. Although Ruhman and co-workers’ Model 2 treats the conversion of the non-equilibrated sodium atom into the 900-nm species as a kinetic rather than a solvation process, both the DE+S model and Model 2 posit that a non-equilibrated precursor to the 900-nm absorbing species forms kinetically from the 590-nm absorbing gas-phase-like sodium atom ( $\text{Na}_{\text{hot}}^0$  or  $\text{Na}_{\text{dry}}^0$ ).<sup>26,37</sup> The most important difference between our DE+S model and Ruhman and co-workers’ Model 2, however, is the way the ejection of the CTTS electron is treated. Our DE+S model assumes that the solvated electron does not appear until after a delay time (which our original fits to the DE+S model gave as  $\sim 700$  fs),<sup>26</sup> whereas Ruhman and co-workers’ Model 2 assumes that the electron is ejected essentially immediately into solution, on a  $\leq 200$  fs time scale.<sup>36,37</sup> It is worth noting, however, that the DE+S model and Model 2 should be able to fit the visible ultrafast spectral transients equally well since both models have the same number of intermediate species and since the solvated electron contributes little to the total transient spectroscopy in the visible region (*cf.* Figure 1). This is why we believe that probing in the IR, where the electron is the sole absorber (*e.g.*, Figure 2), is critical to distinguishing between different kinetic schemes for the  $\text{Na}^-/\text{THF}$  CTTS system.

Ruhman and co-workers have presented several arguments in favor of why the CTTS ejection of the electron from  $\text{Na}^-$  in THF should take place in  $\leq 200$  fs. First, Ruhman and coworkers<sup>36</sup> (as well as our group<sup>26</sup>) have measured the transient spectral dynamics of photoexcited  $\text{Na}^-$  in THF near 1200 nm and found an absorption that appears instantaneously and then decays on a  $\sim 200$ -fs time scale.<sup>72</sup> Ruhman and coworkers have assigned this rapid decay to ejection of the electron from the initially-prepared CTTS excited state.<sup>36,37</sup> Second,

Ruhman and coworkers have argued that if the CTTS ejection were delayed, the excited electron would completely dissipate its excess energy prior to ejection and thus there would be no change in the distribution of electron ejection distances with excitation energy,<sup>36,37</sup> contrary to what is observed.<sup>25-27,35</sup> Finally, Ruhman and co-workers have argued that the instrument-limited appearance of the gas-phase-like Na atom absorption near 590 nm, which is seen for all excitation wavelengths and in all solvents,<sup>34,37</sup> implies that there can be no quantum mechanical correlation between the excited CTTS electron and the electron remaining on the Na atom, and thus that the CTTS electron must be detached even at these very early stages.<sup>37</sup>

In contrast to Ruhman and coworkers, we have argued that the ejection of the CTTS electron is delayed for several reasons. First and foremost, we have directly observed the delayed appearance of the solvated electron's ~2000-nm absorption (Figure 2 and References 25-27). The fact that the spectral kinetics are identical across all the wavelengths where the electron is the sole absorber indicates a delayed growth of the electron population and not dynamic solvation or some other process.<sup>27</sup> Second, we have performed a series of three-pulse experiments in which the Na<sup>-</sup> CTTS transition was excited at 780 nm and the initially-created excited state/detached electron was re-excited at ~2000 nm, with the results probed at 1250 nm.<sup>27,29</sup> By varying the time delay at which the ~2000-nm pulse was applied, we were able to directly map out the dissipation of energy from the CTTS excited state *before* detachment occurred. We found that the energy of the initially-prepared CTTS excited state dissipates relatively slowly, on a ~450-fs time scale,<sup>27</sup> verifying that the electron detachment process must be taking place on an equal or slower time scale. Finally, we agree with Ruhman and coworkers that the correlation between the two sodium anion valence electrons is broken essentially instantaneously upon excitation, explaining why the remaining electron on the Na atom initially has a gas-phase-like absorption regardless of the excitation energy of the CTTS electron. Whether or not the excited CTTS electron initially occupies a localized *p*-like state in the parent cavity following low-energy excitation or a disjoint state that extends across multiple solvent cavities following high-energy excitation, we believe that the excited electron no longer significantly interacts with the electron remaining on the Na atom. Even though correlation between the electrons is likely lost instantaneously, however, we do not define detachment as being complete until the excited CTTS electron reaches its electronic ground state in its new, detached cavity, as seen by the appearance of the solvated electron's (equilibrium) absorption

spectrum. We have argued that the excited CTTS electron, prior to detachment, is what absorbs near 1200 nm, and that the rapid decay seen at this probe wavelength is the result of the ~450-fs dynamic solvation of the excited state that occurs before detachment is complete.<sup>26,27</sup> This solvation is followed by a (delayed) radiationless transition to form the detached, nearly pre-equilibrated ground-state electron, explaining its delayed appearance and lack of solvation.

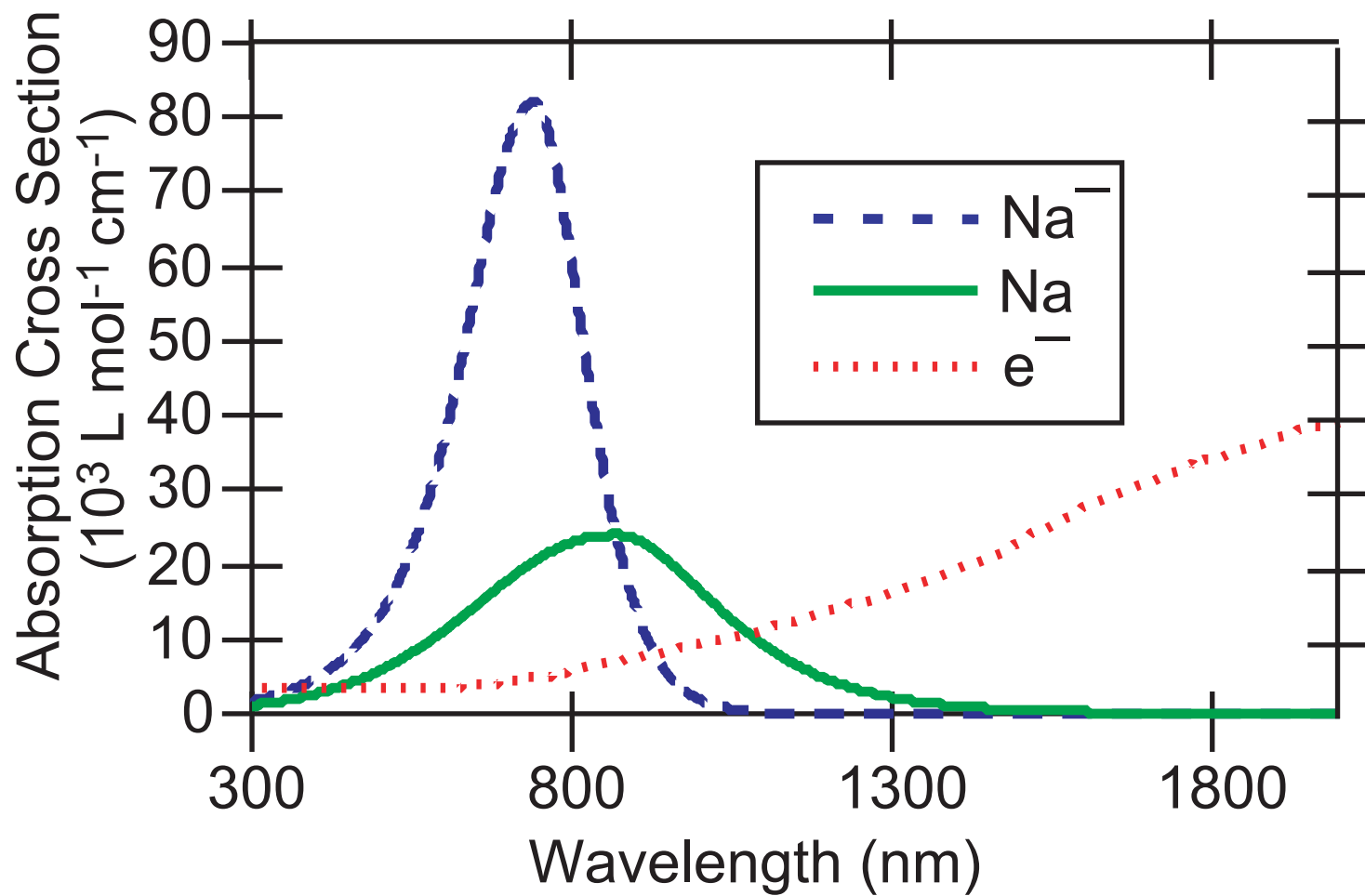
## References:

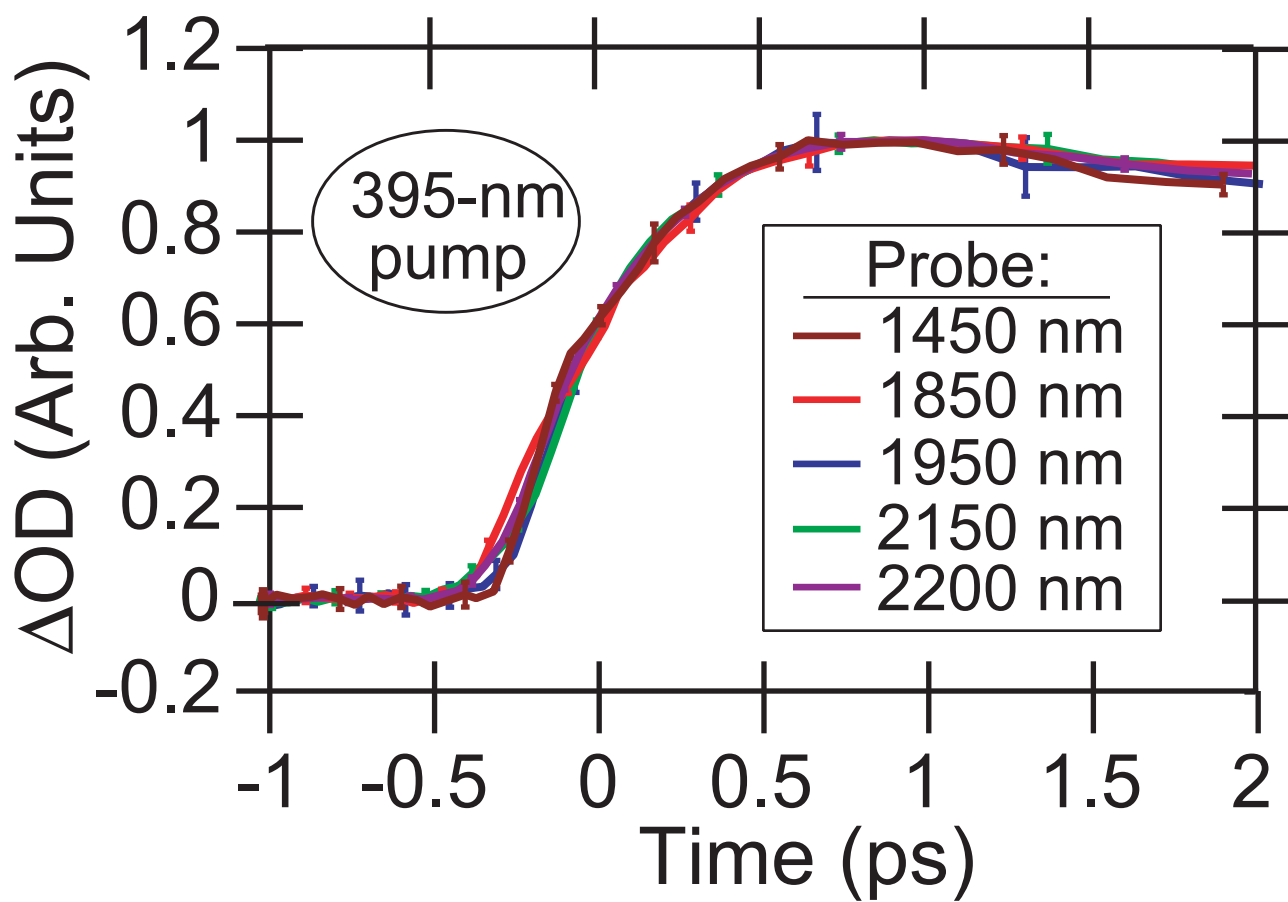
- <sup>1</sup> Maroncelli, M. *J. Mol. Liq.* **1993**, *57*, 1.
- <sup>2</sup> Warshel, A.; and Parson, WW. *Ann. Rev. Phys. Chem.* **1991**, *42*, 279.
- <sup>3</sup> Stratt, R.M.; and Maroncelli, M. *J. Phys. Chem.* **1996**, *100*, 12981.
- <sup>4</sup> Reynolds, L.; Gardecki, J.A.; Frankland, S.J.V.; Gorng, M.L.; and Maroncelli, M. *J. Phys. Chem.* **1996**, *100*, 10337.
- <sup>5</sup> Glasbeek, M.; and Zhang, H.; *Chem. Rev.* **2004**, *104*, 1929.
- <sup>6</sup> de Boeij, W.P.; Pshenichnikov, M.S.; and Wiersma, D.A. *Annu. Rev. Phys. Chem.* **1998**, *49*, 99.
- <sup>7</sup> Lang, M.J.; Jordanides, X.J.; Song, X.; and Fleming, G.R. *J. Chem. Phys.* **1999**, *110*, 5884.
- <sup>8</sup> Cho, M.; and Fleming, G.R.; *Annu. Rev. Phys. Chem.* **1996**, *47*, 109.
- <sup>9</sup> Larsen, D.S.; Ohta, K.; Xu, Q.H.; Cyrier, M.; and Fleming, G.R.; *J. Chem. Phys.* **2001**, *114*, 8008.
- <sup>10</sup> Corbin, R.A.; and Fajardo, M. E. *J. Chem. Phys.* **1994**, *101*, 2678.
- <sup>11</sup> Fajardo, M.E.; and Boatz, J.A. *J. Comput. Chem.* **1996**, *18*, 381.
- <sup>12</sup> Jen, C.K.; Bowers, V.A.; Cochran, E.L.; and Foner, S.N. *Phys. Rev.* **1962**, *126*, 1749.
- <sup>13</sup> Edwards, P. P. *J. Supercond.* **2004**, *13*, 933.
- <sup>14</sup> Tuttle, T.R., Jr. *J. Phys. Chem.* **1975**, *79*, 3071.
- <sup>15</sup> Catterall, R.; and Edwards, P.P. *J. Phys. Chem.* **1975**, *79*, 3010.
- <sup>16</sup> Seddon, W.A.; Fletcher, J.W.; and Catterall, R. *Can. J. Chem.* **1977**, *55*, 2017.
- <sup>17</sup> Catterall, R.; Slater, J.; Seddon, W.A.; and Fletcher, J.W. *Can. J. Chem.* **1976**, *54*, 3110.
- <sup>18</sup> Catterall, R.; Slater, J.; and Symons, M.C.R. *Can. J. Chem.* **1977**, *55*, 1979.
- <sup>19</sup> Seddon, W.A.; Fletcher, J.W.; Sopchyshyn, F.C.; and Catterall, R. *Can. J. Chem.* **1977**, *55*, 3356.
- <sup>20</sup> Bockrath, B; and Dorfman, L.M. *J. Phys. Chem.* **1973**, *77*, 1002.
- <sup>21</sup> Seddon, W.A.; Fletcher, J.W.; Sopchyshyn, F.C.; and Selkirk, E.B. *Can. J. Chem.* **1978**, *57*, 1792.
- <sup>22</sup> Seddon, W.A.; Fletcher, J.W. *J. Phys. Chem.* **1980**, *84*, 1104.

- <sup>23</sup> Lide, D.R. Ed. *CRC Handbook of Chemistry and Physics*, 71<sup>st</sup> ed.; CRC Press: Boca Raton, FL, 1990; p. 10-91.
- <sup>24</sup> Jou F.Y.; and Dorfman L.M.; *J. Chem. Phys.* **1973**, 58, 4715.
- <sup>25</sup> Barthel, E.R.; Martini, I.B.; and Schwartz, B.J.; *J. Chem. Phys.* **2000**, 112, 9433.
- <sup>26</sup> Barthel, E.R.; Martini, I.B.; and Schwartz, B.J. *J. Chem. Phys.* **2003**, 118, 5916.
- <sup>27</sup> Martini, I.B.; and Schwartz, B.J.; *J. Chem. Phys.* **2004**, 121, 374.
- <sup>28</sup> Martini, I.B.; Barthel, E.R.; and Schwartz, B.J. *Science* **2001**, 293, 462.
- <sup>29</sup> Martini, I.B.; Barthel, E.R.; and Schwartz, B.J. *J. Am. Chem. Soc.* **2002**, 124, 7622.
- <sup>30</sup> Barthel, E.R.; and Schwartz, B.J. *Chem. Phys. Lett.* **2003**, 375, 435.
- <sup>31</sup> Martini, I.B.; Barthel, E.R.; and Schwartz, B.J. *J. Chem. Phys.* **2000**, 113, 11245.
- <sup>32</sup> Barthel, E.R.; Martini, I.B.; and Schwartz, B.J. *J. Phys. Chem. B* **2001**, 105, 12230.
- <sup>33</sup> Martini, I.B.; and Schwartz, B.J. *Chem. Phys. Lett.* **2002**, 360, 22.
- <sup>34</sup> Bartel, E. R.; Martini, I. B.; Keszei E.; Schwartz, B. J.; in *Proc. Ultrafast. Phenom. XIII*, Springer Series Chem. Phys. **71**, Miller, R. D.; Murnane, M. M.; Scherer N. F.; Weiner, A. M., Eds. Spinger-Verlag, Berlin (2003), p. 459.
- <sup>35</sup> Martini, I.B.; Barthel, E.R.; and Schwartz, B.J. *Pure Appl. Chem.* **2004**, 76, 1809.
- <sup>36</sup> Wang, Z.; Shoshana, O.; Hou, B.; and Ruhman, S. *J. Phys. Chem. A* **2003**, 107, 3009.
- <sup>37</sup> Shoshana, O.; Pérez Lustres, J.L.; Ernsting, N.P.; and Ruhman, S. *Phys. Chem. Chem. Phys.* **2006**, 8, 2599.
- <sup>38</sup> Dye, J.L. *Prog. Inorg. Chem.* **1984**, 32, 327.
- <sup>39</sup> Dye, J.L. *J Chem. Educ.* **1977**, 54, 332.
- <sup>40</sup> Lok, M.T.; Tehan, F.J.; Dye, J.L. *J. Phys. Chem.* **1972**, 76, 2975.
- <sup>41</sup> Smallwood, C.J.; Bosma, W.B.; Larsen, R.E.; and Schwartz, B.J.; *J. Chem. Phys.* **2003**, 119, 11263.
- <sup>42</sup> We note, however, that the recent experiments by Ruhman and co-workers described in Ref. 37 are not entirely consistent with the CTTS band being composed of three orthogonally-polarized subbands. This is because these workers report a *negative* parallel-minus-perpendicular change in optical density at the spectral position of the highest-energy of the three *p*-like subbands following excitation of the lowest-energy *p*-like subband. Since the highest- and lowest-energy subbands should have orthogonal transition dipoles, the signal measured by Ruhman and co-workers is expected to be positive if the CTTS band is indeed composed of three orthogonally-polarized *p*-like subbands.
- <sup>43</sup> Yu, J.; and Berg, M. *J. Phys. Chem.* **1993**, 97, 1758.
- <sup>44</sup> Cavanagh, M.C.; Martini, I.B.; and Schwartz, B.J. *Chem. Phys. Lett.* **2004**, 396, 359.
- <sup>45</sup> Schwartz, B.J.; and Rossky, P.J. *Phys. Rev. Lett.* **1994**, 72, 3282.

- <sup>46</sup> Bedard-Hearn, M.J.; Larsen, R.E.; and Schwartz, B.J. *J. Chem. Phys.* **2005**, *122*, 134506.
- <sup>47</sup> Bedard-Hearn, M.J.; Larsen, R.E.; and Schwartz, B.J. *J. Chem. Phys.* **2006**, *125*, 194509.
- <sup>48</sup> Bowron, D.T.; Finney, J.L.; and Soper, A.K. *J. Am. Chem. Soc.* **2006**, *128*, 5119.
- <sup>49</sup> Kloepfer, J.A.; Vilchiz, V.H.; Lenchenkov, V.A.; and Bradforth, S.E. *Chem. Phys. Lett.* **1998**, *298*, 120.
- <sup>50</sup> Kloepfer, J.A.; Vilchiz, V.H.; Lenchenkov, Germaine, A.C.; V.A.; and Bradforth, S.E. *J. Chem. Phys.* **2000**, *113*, 6288.
- <sup>51</sup> Vilchiz, V.H.; Kloepfer, J.A.; Lenchenkov, Germaine, A.C.; V.A.; and Bradforth, S.E. *J. Phys. Chem. A* **2001**, *105*, 1711.
- <sup>52</sup> Vilchiz, V.H.; Chen, X.; Kloepfer, J.A.; and Bradforth, S.E. *Radiat. Phys. Chem.* **2005**, *72*, 159.
- <sup>53</sup> Moskun, A.C.; and Bradforth, S.E. *J. Phys. Chem. A* **2006**, *110*, 10947.
- <sup>54</sup> Nguyen, T.-Q.; Martini, I.B.; and Schwartz, B.J. *J. Phys. Chem. B* **2000**, *104*, 237.
- <sup>55</sup> The zero of time was also allowed to vary in the fitting for each probe wavelength.
- <sup>56</sup> We note that Reference 24 does not present any cross-section data for the solvated electron that is blue of 557 nm, so for wavelengths bluer than this, we assumed that the electron absorption is flat. As discussed in detail in the Supplementary Information, this should be a good approximation and it has a negligible effect on our final results.
- <sup>57</sup> As will be discussed further in the conclusions as well as in reference 26, there is a possibility that the excited CTTS electron could also absorb to some extent in this region.
- <sup>58</sup> We note that in this spectral region, there is no distinction between the DE model presented in Ref. 25 and the DE+S model presented in Ref. 26. See the Appendix for details.
- <sup>59</sup> Although we are unable to test this assumption since there is no wavelength where we can cleanly probe the bleach, we feel this assumption is reasonable since the sodide CTTS band is expected to have a very similar electronic structure to the hydrated electron, where there is no dynamic solvation seen in the bleach. See Refs. 43, 44, and 45
- <sup>60</sup> We would expect to see spectral diffusion if the experiments were not done with the pump and probe pulses set to magic angle since we know there is a probe wavelength dependence to the anisotropy in the bleach.<sup>26,36,37</sup>
- <sup>61</sup> In Ref. 37, Ruhman and co-workers did not divide out the population dynamics in their analysis since they assumed that there was no recombination and thus that the sodide bleach did not have any population dynamics.
- <sup>62</sup> Hendler, R.W.; and Shrager, R.I. *J. Biochem. Biophys. Methods* **1994**, *28*, 1.
- <sup>63</sup> Since our data was collected at discrete energies, we numerically integrated to obtain the average frequency using the midpoint rule.
- <sup>64</sup> We chose to use Lorentzians for these fits since the high-energy side of the ( $\text{Na}^+, e^-$ ) species fits well to a Lorentzian and since we only have collected the high-energy part of the spectrum during this solvation process.

- <sup>65</sup> This rise time is not identical to the average solvation time because it reflects only the time it takes the ( $\text{Na}^+, e^-$ ) spectrum to grow in at this wavelength.
- <sup>66</sup> Bedard-Hearn, M.J.; Larsen, R.E.; and Schwartz, B.J. *J. Phys. Chem. B* **2003**, *107*, 14464.
- <sup>67</sup> Ruhman and coworkers also missed this slower solvation time in their most recent work exciting  $\text{Na}^-$  at 400 nm because they assumed the spectrum had reached equilibrium by  $\sim 4$  ps; see the Supplementary Information for more details.
- <sup>68</sup> This solvation process is likely not due to cooling of the sodium atom since it is well-known that the CTTS bands of solutes shift to the blue upon cooling [Ref. 40] whereas the spectrum of the Na atom that we observe undergoes a dynamic red-shift.
- <sup>69</sup> As documented in Ref. 4, the long-time solvation component seen for coumarin 153 in liquid THF is  $\sim 1$  ps.
- <sup>70</sup> Bragg, A.E.; and Schwartz, B. J.; manuscript in preparation.
- <sup>71</sup> When we employed this model in our original paper (Ref. 25), we assumed the solvent-separated and free electrons did not decay since the decay of both of these species is at least an order of magnitude longer than the  $\sim 10$ -ps dynamics that we were fitting to the model. In the version of the model employed in this paper, we assumed that the solvent-separated and free electrons recombined on the same (hundreds of ps) time scale, accounting for the small amount of longer-time recombination on the  $\sim 40$ -ps time scale being considered.
- <sup>72</sup> Although the experiments done by the Ruhman group have a faster time resolution than the experiments done in our group ( $\sim 60$  fs vs  $\sim 120$  fs), no dynamics have been observed in this system that are faster than the  $\sim 200$  fs decay seen at  $\sim 1200$  nm. Therefore, even with our slower time resolution, we are able to observe all the dynamics associated with the sodide CTTS process.





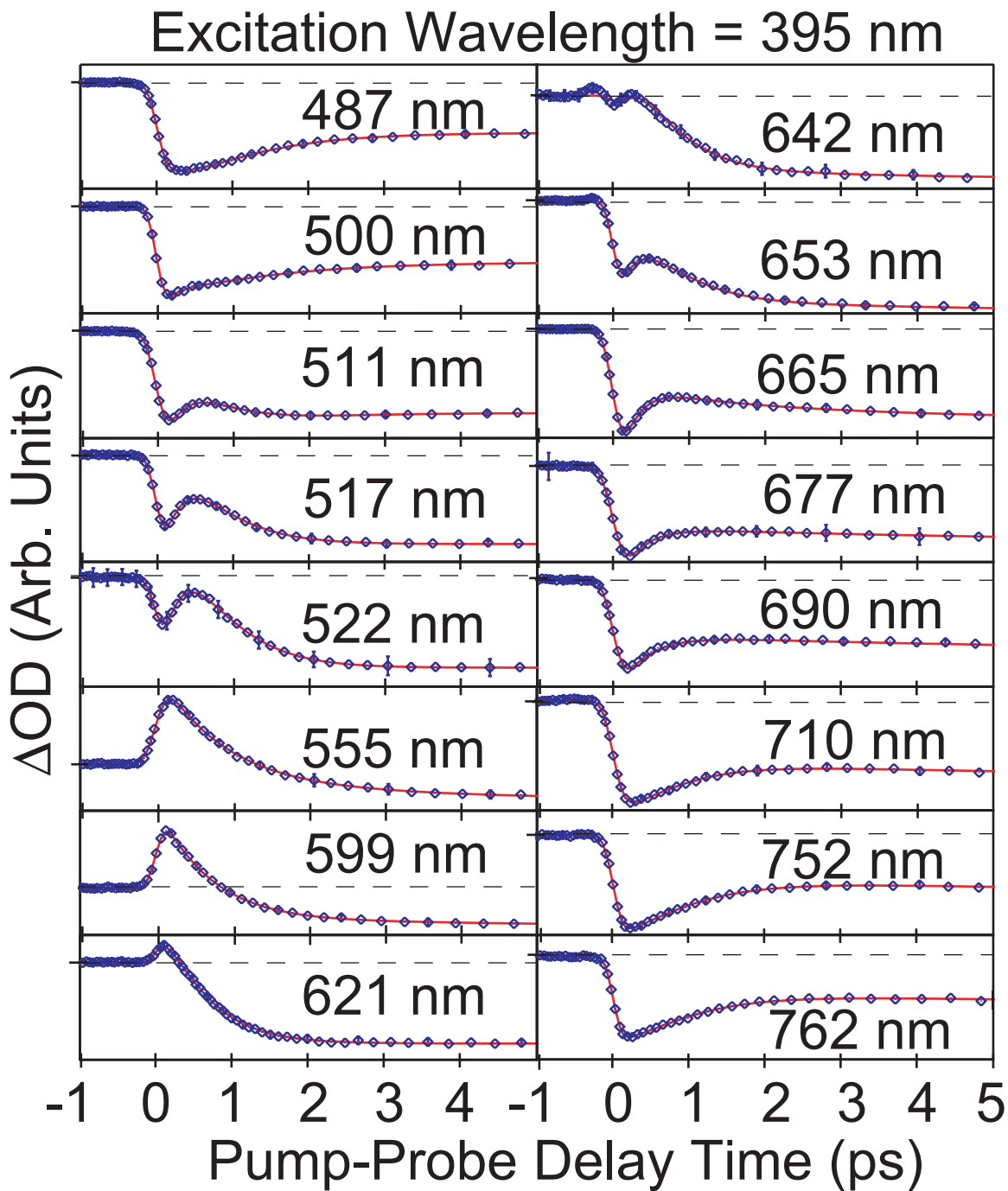


Figure 3, Cavanagh, et al.

